HHS Public Access

Author manuscript

J Immunol. Author manuscript; available in PMC 2016 April 01.

Published in final edited form as:

J Immunol. 2015 April 1; 194(7): 3147–3155. doi:10.4049/jimmunol.1402739.

Therapeutic regulatory T cells subvert effector T cell function in inflamed islets to halt autoimmune diabetes[1]

Ashley E. Mahne, **Joanna E. Klementowicz**, **Annie Chou**, **Vinh Nguyen**, and **Qizhi Tang**

Department of Surgery, University of California, San Francisco, 513 Parnassus Ave., San Francisco, CA 94143

Abstract

Therapeutic regulatory T cells (Tregs) can reverse pre-established autoimmune pathology. In this study, we aimed to determine the means by which therapeutic Tregs control islet inflammation using a mouse model of autoimmune diabetes. Islet antigen-specific Tregs infiltrated inflamed islets soon after infusion into pre-diabetic mice, which was quickly followed by a selective reduction of mRNA associated with effector T cells in the islets. This change was partially due to decreased $CD8^+$ T cell accumulation in the tissue. $CD8^+$ T cells that remained in the islets after Treg treatment were able to engage dendritic cells in a manner similar to that found in untreated mice, consistent with the retention of an activated phenotype by islet dendritic cells shortly following Treg treatment. Nonetheless, Treg treatment abrogated IFNγ production by intra-islet $CD8^+$ and $CD4^+$ T cells at the protein level with minimal effect on IFNγ mRNA. Sustained expression of IFNγ protein by effector T cells was dependent on common γ chain cytokine activation of the mTOR pathway, which was suppressed in islet $CD8^+$ T cells *in vivo* following Treg treatment. These multifaceted mechanisms underlie the efficacy of therapeutic Treg subversion of effector T cell functions at the site of inflammation to restore normal tissue homeostasis.

Introduction

Regulatory T cells (Tregs) are essential for maintaining immune homeostasis and preventing autoimmune diseases. Treg control of immune responses can be divided into three distinct phases: homeostatic control, damage control, and infectious tolerance (1). Treg prevention of dendritic cell (DC) activation in lymphoid organs is important in the maintenance of immune homeostasis and prevention of self-reactive T cell priming (2, 3). In an ongoing immune response when T cell priming is established, such as in the setting of chronic autoimmune diseases, Tregs must act in the target tissues to mitigate further damage by pre-activated cells. In this context, Tregs have been found to suppress established $CD4^+$ T cell-mediated inflammation in the intestine (4, 5). These studies have shown that Tregs can suppress further T cell proliferation and activation, as well as effector T cell survival,

[1]This work was supported by grants from the National Institutes of Health R01 DK08231 (Q.T.), P30 DK063720 UCSF Diabetes and Endocrinology Research Center, the UCSF PBBR program (Q.T.), and generous support by the Coates family.

Address correspondence to: Dr. Qizhi Tang, 513 Parnassus HSE-520, Box 0780, San Francisco, CA 94143, Tel: (415) 476-1739, Fax: (415) 502-8326, qizhi.tang@ucsfmedctr.org.

migration into the target tissue or their function. Tregs have also been shown to suppress $CD8^+$ T cell degranulation and killing of target cells *in vivo* (6). Once inflammatory tissue destruction is under control, Tregs can impart regulatory properties onto other cells in a process called infectious tolerance for long-term immune quiescence (7, 8).

Type 1 diabetes is a highly localized, tissue-specific autoimmune disease, and research in the non-obese diabetic (NOD) mouse has demonstrated that Treg function and impairments are highly localized to the inflamed islets (9, 10). Moreover, infusion of islet-antigen-specific Tregs from TCR transgenic NOD.BDC2.5 mice can prevent and reverse diabetes (11, 12). In a recent report, autologous Treg therapy stalled the progressive decline of c-peptide in children with new onset type 1 diabetes (13). Understanding how therapeutic Tregs control disease progression may help to optimize Treg cell therapy and shed light on the pathogenic mechanisms that drive disease progression. While the effects of Treg therapy in the draining pancreatic lymph node (PLN) have been previously reported (14), in this work we sought to elucidate the primary impacts of therapeutic Tregs in the suppression of an ongoing immune response in the target tissue itself, the pancreatic islets. In doing so, we have identified distinct mechanisms by which Tregs control effector T cells in inflamed islets.

Materials and Methods

Mice

NOD.$CD28^{-/-}$, NOD.CD11c-YFP.$CD28^{-/-}$, NOD.$Foxp3^{DTR+}$ (15), NOD.BDC2.5.Thy1.1 TCR transgenic, NOD.uGFP.BDC2.5.Thy1.1 TCR transgenic, and NOD.8.3.Thy1.1 TCR transgenic mice were housed and bred at the UCSF Animal Barrier Facility. The UCSF IACUC approved all experiments.

qRT-PCR

Islets were isolated as previously described (16). Whole islets or sorted cells were lysed in TRIzol (Invitrogen). RNA was extracted using RNeasy Micro columns (QIAGEN). Reverse transcription was done using SuperScript III (Invitrogen). qRT-PCR SYBR Green Mastermix and primers were from QIAGEN and reactions were run on a CFX 96 (Bio-Rad). An RT^2 Profiler Custom PCR Array (QIAGEN) was used for whole islet experiments.

Immunofluorescence microscopy

Pancreas cryosections were fixed in 4% PFA and stained with anti-phospho-S6 ribosomal protein (2F9; Cell Signaling Technology), anti-CD8, anti-CD4, and DAPI (Invitrogen). Images were acquired on a Leica SP5 confocal microscope using a 63× water immersion objective. Acquisition and post-acquisition analyses and visualization were performed using Leica Application Suite Advanced Fluorescence Lite software and Imaris software (Bitplane AG). T cells were enumerated using Imaris or manually by a blinded party unaware of the treatment conditions. Enumerating the number of $pS6^+$ T cells was done manually by a person blinded to the experimental conditions.

Two-photon microscopy

Islets were stained with Hoechst for 15 min at room temperature and embedded in RPMI containing 0.5% low melting point agarose (Invitrogen). Embedded islets were imaged on a custom-built two-photon microscope as previously described (14). For time-lapse image acquisition, *z*-stacks with up to 40 *xy* planes with 5 um spacing were acquired every 30 or 60 s for 20–60 min. Data were visualized and analyzed using Imaris software.

Flow cytometry

Islet and LN single cell suspensions were prepared as previously described (16). The following antibodies were used to stain the cells: anti-CD4-PE (RM4-5), anti-CD8-Pacific orange (5H10), anti-CD45-APC-Cy-7 (30-F11), anti-Thy1.1-PerCP (OX-7), anti-Thy1.2-AL700 (30H12), anti-B220-Pacific blue (RA3-6B2), anti-CD11c-PE-Cy7 (N418), anti-Ki67-FITC (SolA15), anti-Bcl2-PE (3F11), anti-IAg7-AL700 (10-2.16), anti-CD40-PE (3/23), anti-CD80-biotin (16-10A1), anti-PD-1-FITC (J43) and anti-CD86-APC (GL-1). For intracellular cytokine staining, PLN cells were restimulated *in vitro* with 10 ng/ml PMA and 0.5 μM ionomycin in the presence of 10 μg/ml Brefeldin A (BFA, Sigma Aldrich) for 2–3 hours. For direct *ex vivo* intracellular cytokine staining in islet T cells, *in vivo* BFA treatment was adapted from a previously published method (17). Mice were i.v. injected with 250 μg BFA 4 h prior to sacrifice. Islet isolation was done with the addition of 10 μg/ml BFA throughout. Islets were cultured at 37° for an additional 2 h in RPMI with BFA and dissociated in the presence of BFA. For both PLN and islet cells, cells were fixed with 4% PFA for 5 min at room temperature after surface staining. Fixed cells were permeabilized in 0.1% saponin and stained with anti-IFNγ (XMG1.2; eBioscience). Analyses were performed on a LSRII or Fortessa flow cytometer (BD Biosciences) with FACSDiva analysis software (BD Biosciences).

Cell transfers

Tregs from NOD.BDC2.5.Thy1.1 or NOD.uGFP.BDC2.5.Thy1.1 TCR transgenic mice were FACS-sorted to high purity (>99%) and expanded as previously described (11). 10^6 expanded BDC2.5 Tregs were transferred to pre-diabetic mice via i.p. injection, or in the case of two photon experiments, via i.v. injection. $CD8^+$ T cells were enriched from spleens of NOD.8.3.Thy1.1 TCR transgenic mice using biotinylated antibodies against CD4, CD19, and CD11b followed by depletion with Dynabeads Biotin Binder (Invitrogen). $CD4^+CD25^-$ BDC2.5 T cells were negatively selected from spleens of NOD.BDC2.5.Thy1.1 TCR transgenic mice using antibodies against CD8, CD25, CD19 and CD11b. For two photon experiments, enriched $CD8^+$ T cells were labeled with CMTMR or CFSE (Invitrogen) and $8–10 \times 10^6$ cells were injected i.v. For *in vivo* proliferation and cytokine experiments, bead-enriched cells were further negatively sorted by FACS to high purity, labeled with CFSE, and 10^6 of each cell type was injected i.v.

Ex vivo islet cell culture and phosphoflow

Dissociated islet cells were incubated overnight at 37°C in RPMI + 10% FCS in a 96 well U-bottom plate with $2–3 \times 10^5$ cells per well. Anti-CD25 (clone 3C7) was added at 10 μg/ml. Rapamycin was added at 100 ng/ml. Tofacitinib (Selleckchem) was added at 10 μM.

IFNγ concentrations in supernatants were measured using ELISA. Cells were stained with a fixable viability dye (eBioscience), fixed in Lyse/Fix buffer (BD Biosciences), permeabilized in Perm buffer III (BD Biosciences), and stained according to manufacturer's instructions.

In vivo Treg depletion

15- to 17-week-old female NOD.Foxp3^{DTR+} mice and transgene-negative control littermates were injected i.p. with 40ng/g body weight diphtheria toxin (DT, Sigma) on two consecutive days and analyzed 1 day following the second injection (15).

Statistical analysis

Statistical analyses were performed with the aid of Prism software (GraphPad).

Results

Tregs traffic to inflamed islets where they down-regulate an effector T cell signature

We utilized NOD mice deficient in the costimulatory molecule CD28 (NOD.CD28$^{-/-}$), which develop diabetes more rapidly than their wild-type counterparts with 100% penetrance by 12 weeks of age, primarily due to their deficiency in Tregs (18). BDC2.5 Treg treatment of prediabetic NOD.CD28$^{-/-}$ mice at 5 to 7 weeks of age confers 100% long-term protection against diabetes development (11). The stark contrast in disease outcomes between Treg-treated and untreated NOD.CD28$^{-/-}$ mice offers an ideal *in vivo* setting in which to study Treg function in the control of a multifaceted, polyclonal T cell-mediated autoimmune disease. BDC2.5 Tregs rapidly trafficked to the islets within 18 hours of i.v. infusion into 5 to 6 week old NOD.CD28$^{-/-}$ mice, in agreement with a previous report that inflamed islets can directly recruit T cells from the circulation without the cells needing to pass through the draining pancreatic lymph node (PLN) (19). Tregs preferentially trafficked to infiltrated islets over non-infiltrated ones, as greater numbers of Tregs were observed in islets with more severe insulitis, regardless of the time point analyzed (Fig. 1A). Upon arrival, BDC2.5 Tregs were seen to make dynamic interactions with a continuous network of islet DCs (Supplemental Video 1). BDC2.5 Tregs persisted long-term in the islets, where they proliferated and maintained high levels of Foxp3 (Supplemental Fig. 1). However, they did not completely clear insulitis (Fig. 1B). Despite this, none of the treated NOD.CD28$^{-/-}$ mice progress to overt diabetes ((11) and data not shown).

To examine how therapeutic Tregs gain control over the immune infiltrate, we developed a qRT-PCR array that contained genes relevant to the immunopathology of type 1 diabetes, including: indicators of β cell function, markers of immune cell populations, and molecules associated with immune effector functions (Supplemental Table 1). We analyzed whole islet mRNA from NOD.CD28$^{-/-}$ mice at the time of BDC2.5 Treg treatment and at 3 and 7 days following treatment, along with islet mRNA from age-matched untreated littermate controls. Untreated mice showed a progressive decline of insulin expression, demonstrating rapidly advancing β cell destruction in these mice (Fig. 1C). In contrast, mRNA for both insulin 1 and insulin 2 genes was preserved and showed a trend of increase in Treg-treated mice when compared to baseline.

The most notable change in immunological genes at 3 days post-Treg treatment was a downregulation of granzyme A and granzyme B mRNA (Fig. 1D), which became more pronounced at 7 days post-Treg transfer, along with a reduction in IFNγ and the chemokines Cxcl9 and Xcl1 (Fig. 1E). Genes upregulated at 7 days post-Treg treatment included the immunosuppressive cytokine IL-10, as well as IL-6, which has been shown to have direct cytoprotective effects on β cells and to improve β cell function (20, 21). NK cells express granzymes and IFNγ, and have been implicated to be a primary Treg target in BDC2.5 TCR transgenic mice (15). Consistent with this previous report, we found that the NK cell marker Klrd1 was also reduced after Treg treatment (Fig. 1E). However, NK cells, which exhibit functional and numeric defects in NOD mice (22, 23), made up on average less than 2% of the total immune cell infiltrate. In contrast, $CD8^+$ T cells represented an average of about 10% of the immune infiltrate (data not shown). CD8α was reduced 5.3-fold 7 days after Treg treatment (Fig. 1E), while markers for other major cell populations remained relatively unchanged (Supplemental Table 1). The reduction of CD8α mRNA could not be attributed to a decrease in $CD8^+$ DCs because DCs in inflamed islets were predominantly $CD11b^+CD8\alpha^-$ (16). Altogether, these changes implicated cytotoxic $CD8^+$ T cells as the cells immediately impacted by Treg therapy in inflamed islets.

Tregs reduce $CD8^+$ T cell accumulation in the islets

We next enumerated intra-islet $CD8^+$ T cells using immunofluorescence microscopy in pancreas sections from NOD.$CD28^{-/-}$ mice at 7 days post-Treg treatment and in age-matched controls. Significantly fewer $CD8^+$ T cells per islet section were observed in Treg-treated mice than in controls (Fig. 2A). This decrease in $CD8^+$ T cells was not due to a decrease in $CD8^+$ T cell proliferation, as measured by Ki67 expression (Fig. 2B), or decreased expression of the prosurvival protein Bcl2, measured as the median fluorescence intensity of Bcl2 protein in $CD8^+$ T cells (Fig. 2C), or by the percentage of $Bcl2^+$ cells (data not shown). In addition, we examined expression of the exhaustion marker PD-1 and found that Treg treatment moderately decreased PD-1 expression on $CD8^+$ T cells (Fig. 2D). Together, these data indicated that the reduced numbers of islet $CD8^+$ T cells was likely caused by factors other than reduced *in situ* expansion and survival of $CD8^+$ T cells.

$CD8^+$ T cells utilize the chemokine receptor Cxcr3 to home to sites of inflammation in multiple disease settings (24). Since peripheral $CD8^+$ T cells in NOD mice express Cxcr3 (Supplemental Fig. 2), and one of its ligands, Cxcl9, was reduced in the islets after Treg treatment (Fig. 1D), we assessed if Treg treatment inhibited $CD8^+$ T cell trafficking to the islets. Using two-photon microscopy, we examined the overnight islet accumulation of adoptively transferred 8.3 $CD8^+$ T cells, which express a transgenic TCR that is specific for the β cell antigen IGRP (25). Significantly fewer 8.3 T cells were seen within the islets of NOD.$CD28^{-/-}$ mice that had been treated with Tregs 7 days prior than in the islets of age-matched control mice (Fig. 2E). Together, these data suggest that the reduction in islet $CD8^+$ T cells observed histologically and by qPCR profiling was due in part to reduced recruitment and/or decreased retention shortly following their arrival in the tissue.

Treg treatment does not inhibit islet T cell-DC interactions

While Treg treatment significantly reduced $CD8^+$ T cell accumulation in the islets, large numbers of $CD8^+$ T cells persisted, along with the rest of the islet immune infiltrate (Fig. 2A). DCs are essential for sustaining inflammation in the islets (26, 27), and we have previously shown that islet infiltration by T cells leads to massive recruitment and activation of DCs, which amplifies the autoimmune response (16). Additionally, other studies have implicated DCs as targets of Treg suppression (3, 28). Therefore, we tested the hypothesis that Tregs control $CD8^+$ T cells indirectly by suppression of DCs.

Intra-islet DCs largely maintained an activated profile 7 days after Treg treatment; with high levels of expression of MHC class II and CD80 that were comparable to age-matched untreated NOD.$CD28^{-/-}$ littermates (Fig. 3A). Expression of CD86 and CD40 on islet DCs was moderately and significantly decreased in Treg-treated mice (Fig. 3A); however, despite these decreases, expression levels of these molecules on Treg-treated islet DCs remained as high as or higher than the levels observed on DCs in the draining PLN.

We and others have previously shown that Tregs inhibit DC interactions with effector T cells in the lymph nodes, thereby preventing their activation (14, 29). To determine if Treg treatment altered the ability of DCs to activate $CD8^+$ effector T cells in the inflamed islets, we transferred dye-labeled 8.3 $CD8^+$ T cells into NOD.$CD28^{-/-}$.CD11c-YFP mice 7 days after BDC2.5 Treg infusion and performed time-lapse imaging of isolated islets the next day using two-photon microscopy. Significantly fewer 8.3 T cells were present in the islets of Treg-treated mice following the overnight transfer when compared to cells in age-matched controls (Fig. 2E). However, all 8.3 T cells that entered the islets of Treg-treated mice actively engaged DCs in a manner comparable to 8.3 T cells in untreated control islets (Fig. 3B and Supplemental Videos 2 and 3). Quantification of 8.3 T cell dynamics showed similar velocities of 8.3 T cells in the presence and absence of BDC2.5 Tregs (Fig. 3C). Additionally, we observed that $CD8^+$ T cells were significantly more confined in the presence of BDC2.5 Tregs, as measured by their confinement ratios (the ratio of the displacement and the total distance travelled by a cell) (Fig. 3D). These results demonstrate that Tregs did not disrupt T cell-DC interactions in the inflamed islets despite the slight decrease of CD86 and CD40 expression following Treg treatment.

Tregs suppress islet T cell effector function

We next determined the functional impacts of Treg treatment on islet effector T cells. We adoptively co-transferred 8.3 $CD8^+$ and BDC2.5 $CD4^+CD25^-$ T cells into NOD.$CD28^{-/-}$ mice that had been treated with BDC2.5 Tregs 3 days prior and analyzed the proliferation and cytokine production of the transferred T cells 4 days later.

In agreement with our previous findings (14), Treg treatment inhibited proliferation of transferred T cells in the PLN (Supplemental Fig. 3A and B). Additionally, transferred T cells in the PLN produced less IFNγ upon *ex vivo* restimulation, indicating an inhibition of activation of newly arrived effectors in the PLN (Supplemental Fig. 3C). However, among endogenous T cells in the PLN, Treg treatment did not diminish the frequency of IFNγ-

competent cells, but rather increased it (Supplemental Fig. 3D). We suspect this to be due to a build-up of previously differentiated effector T cells in the PLN following Treg treatment.

In contrast to the PLN, transferred T cells in the islets proliferated extensively, regardless of BDC2.5 Treg treatment (Fig. 4A and B), consistent with the lack of change in islet T cell Ki67 expression (Fig. 2B) or in islet T cell-DC dynamics (Fig. 3B) following Treg treatment. BDC2.5 T conventional (T_{conv}) cells showed no differences in proliferation in the presence of BDC2.5 Tregs, whereas a moderate attenuation of 8.3 T cell proliferation was observed. Overall, this inhibition in the tissue was slight when compared to that observed in the draining PLN. These results suggest that while the primary impact of Tregs in the lymph node is the suppression of T cell clonal expansion and priming, the Tregs at the site of inflammation largely do not inhibit T cell activation.

Distinct from T cells in the PLN that did not produce detectable IFNγ protein without *in vitro* restimulation (**data not shown**), islet T cells readily expressed IFNγ *ex vivo* after short-term *in vivo* Brefeldin A treatment and without *in vitro* restimulation. Despite their robust proliferation in the tissue, we observed a near total inhibition of IFNγ production by both transferred 8.3 and BDC2.5 T cells in Treg-treated mice, while transferred T cells in islets of untreated littermate controls made considerable amounts of the protein (Fig. 4C). Importantly and in contrast to the PLN, IFNγ expression in endogenous islet T cells was also significantly suppressed in Treg-treated mice (Fig. 4D). Surprisingly, qPCR analysis of $CD8^+$ and $CD4^+$ T cells FACS-purified from Treg-treated islets showed that these cells expressed similar amounts of IFNγ mRNA when compared to cells isolated from untreated control mice (Fig. 4E). This suggests that the downregulation of IFNγ observed at the level of total islet RNA is due to decreased total numbers of islet effector T cells, in agreement with Figure 2. Furthermore, islet T cells that persist in Treg-treated mice appear to be similar to anergic cells that express cytokine mRNA but not protein (30). These results show that Tregs in the target tissue can block effector T cell function at the final stage of effector cytokine protein production.

Tregs suppress mTOR signaling in islet $CD8^+$ T cells that is critical for IFNγ production

Previous studies have shown that T cell anergy can result from inhibition of mTOR signaling (31), and activation of the mTOR pathway is critical in the generation and maintenance of effector cell differentiation (32–36). To determine the requirement for mTOR signaling in sustaining islet T cell effector function, we treated *ex vivo* islet cell cultures with rapamycin, a pharmacological inhibitor of mTOR. Phosphorylated ribosomal S6 protein (pS6), an indicator of active mTOR signaling (37), could be readily detected in islet $CD8^+$ and $CD4^+$ T cells following overnight culture (Fig. 5A). Addition of rapamycin to the culture strongly inhibited pS6, along with a significant reduction of IFNγ (Fig. 5B), demonstrating that mTOR signaling was required for maintaining IFNγ production by effector T cells from inflamed islets.

mTOR activation occurs downstream of PI3K/AKT signaling, which can be triggered by cytokines (37). As Tregs have been shown to suppress effector cells through deprivation of IL-2 (38), we examined the effects of blocking IL-2 signaling on mTOR activation and IFNγ production. Blocking the high affinity IL-2 receptor CD25 moderately reduced pS6 (Fig

5C), which was associated with a moderate reduction of IFNγ (Fig. 5D). This suggests that maintenance of IFNγ production is partially dependent on continued IL-2 signaling. IL-7, another common γ chain cytokine, has been shown to be important for promoting effector and memory T cells in inflamed islets (39). Therefore, we further determined if blocking all common γ chain cytokine signaling would have a stronger impact on IFNγ secretion. We cultured islet cells in the presence of a Jak3 inhibitor, tofacitinib, which led to downregulation of pS6 signaling (Fig. 5E) and blocked IFNγ production (Fig. 5F). To determine if Treg treatment suppressed IFNγ production by blocking mTOR signaling *in vivo*, we examined pS6 protein in intra-islet $CD4^+$ and $CD8^+$ T cells using *in situ* immunofluorescence. Treg treatment led to a significant reduction in $pS6^+$ $CD8^+$ but not $pS6^+$ $CD4^+$ T cells in the inflamed islets (Fig. 5G). Taken together, these results demonstrate that sustained IFNγ secretion by intra-islet effector cells requires constant common γ chain cytokine stimulation and activation of mTOR signaling. Treg therapy blocked mTOR signaling in islet $CD8^+$ T cells, likely through cytokine deprivation.

Lastly, to determine if endogenous Tregs present in the NOD mice functioned in a similar manner to the BDC2.5 Tregs, we examined effector T cell number, IFNγ production, and pS6 expression in NOD mice upon acute depletion of endogenous Tregs. Following 2 days of diphtheria toxin (DT) treatment in NOD.$Foxp3^{DTR+}$ mice, endogenous Tregs were extensively diminished in peripheral lymphoid organs and in the islets as previously reported ((15) and data not shown). We found a trend towards an increase of islet $CD8^+$ T cell numbers in Treg-depleted mice, while $CD4^+$ T cells decreased in number, likely reflecting the depletion of $CD4^+$ Tregs (Fig. 6A). Endogenous islet T cells, both $CD4^+$ and $CD8^+$, increased their IFNγ production following Treg depletion (Fig. 6B). Furthermore, a significant increase in the number of islet $CD8^+$ T cells expressing pS6 was observed. This increase in pS6 was again specific to $CD8^+$ T cells, as no similar increase was observed in $CD4^+$ T cells (Fig. 6C). These results complement the findings from CD28-deficient NOD mice treated with BDC2.5 Tregs to suggest that Tregs suppress islet destruction primarily by controlling $CD8^+$ T cell accumulation and effector T cell functions in the inflamed islets.

Discussion

In this study, we investigated impact of therapeutic Tregs on ongoing chronic autoimmune responses *in vivo*. We found that Tregs preferentially traffic to sites of more severe inflammation. The immediate impact of Tregs in inflamed islets is primarily on $CD8^+$ T cells by reducing their recruitment and rapidly suppressing IFNγ protein production without altering IFNγ mRNA on a per cell basis.

This study highlights the differences in Treg control of an autoimmune response in the target tissue versus the draining lymph node. While Tregs have previously been shown to suppress T cell proliferation and differentiation in the LN, the current work demonstrates that therapeutic Tregs can suppress previously differentiated effector T cells at the site of inflammation to halt further destruction of the tissue. Given the acuteness of the changes in effector molecule expression after Treg treatment, we believe this rapid reversal of effector function happens primarily in the inflamed islets early after Treg treatment. The suppression

in the PLN may complement the effects of Tregs in the tissue by reducing the supply of primed T cells so that long-term immune quiescence is maintained.

In prediabetic mice and patients newly diagnosed with type 1 diabetes, islets are infiltrated by activated inflammatory cells, particularly cytotoxic $CD8^+$ T cells that accumulate with disease progression (40–42). Prompt subversion of T cell effector function may underlie the efficacy of Treg therapy in preserving the function of the target tissue. In NOD.$CD28^{-/-}$ mice, the critical role of $CD8^+$ T cells in disease pathogenesis is demonstrated by the protection against disease onset observed when $CD8^+$ T cells are depleted in mice with established islet insulitis by antibody treatment (data not shown). Our lab has also found inhibition of $CD8^+$ T cells to be the primary effect of therapeutic Tregs in a mouse model of islet transplantation (43). Recent work by others has shown the importance of Treg suppression of NK cells (44–46). In particular, Treg depletion in NOD.BDC2.5.$Foxp3^{DTR+}$ mice leads to rapid diabetes due to activation of NK cells in the pancreas (15, 46). As the BDC2.5 mice express a $CD4^+$ TCR transgene, few $CD8^+$ T cells are present in these mice. This difference may account for the difference in the primary cytotoxic effectors (NK cells versus $CD8^+$ T cells) in our two studies. Nonetheless, both studies emphasize the importance of Treg suppression of cytotoxic effectors in the control of an autoimmune response.

Clues to the mechanism behind our observed discrepancy between persistent IFNγ mRNA expression but lack of IFNγ protein in islet T cells of Treg-treated mice may come from recent work from Pearce and colleagues demonstrating a direct requirement for aerobic glycolysis for translation of IFNγ mRNA but not for cell proliferation or survival of $CD4^+$ T cells (47). This work elegantly showed that GAPDH, an enzyme involved in aerobic glycolysis, binds to and suppresses translation of IFNγ mRNA when its enzymatic activity is not employed. While mTOR is a known regulator of aerobic glycolysis, this process was independent of mTOR signaling in the $CD4^+$ T cells studied by Chang et al. Studies in $CD8^+$ T cells have shown a requirement for mTOR activity and aerobic glycolysis to maintain effector cell differentiation (34–36), consistent with our finding that mTOR signaling is required to sustain the effector function of intra-islet $CD8^+$ T cells. This may help to explain why the inhibition of mTOR activation in our system was specific for $CD8^+$ T cells only, despite the fact that Tregs inhibited effector function of both $CD4^+$ and $CD8^+$ T cells and points to differential signaling requirements between these two cell types. While only a small subset of $CD8^+$ cells were seen to express pS6 at any given time, we consider this to be due to the non-synchronous nature of cell signaling in this *in vivo* system as opposed to population heterogeneity. We believe our study is the first to show that Tregs suppress $CD8^+$ effector T cells via modulation of their metabolism and that this opens a new area meriting further investigation.

A number of external stimuli, including TCR ligation, costimulation, cytokines, and nutrients, can activate mTOR signaling. Surprisingly, we found minimal impact of Treg therapy on islet DC phenotype or their ability to engage T cells at this early time point. Thus, while not definitively ruled out, it is unlikely that the observed disruption in mTOR signaling is due to inhibition of TCR or costimulatory signals. Inhibition of cytokine signaling, particularly IL-2 deprivation, has been shown by others to be a mechanism by which Tregs can suppress $CD4^+$ T cells (48), NK cells (45, 46) and even $CD8^+$ T cells (38).

Here we have shown that common γ chain cytokine signaling is required for mTOR signaling and continued IFNγ production by islet effector cells. Thus, our results are consistent with the notion that Treg suppression of effector cells in inflamed islets is mediated by alterations in common γ chain cytokine signaling.

Overall, we have demonstrated that Tregs function efficiently at the site of inflammation at multiple levels to halt tissue destruction by subverting fully differentiated effector T cells. In addition to their homeostatic function to suppress T cell priming in the draining lymph node (14), Tregs exert damage control in the inflamed tissue by inhibiting the accumulation of effector cells and by repressing effector function in fully differentiated T cells. This multi-functional capacity of Tregs is likely critical for their remarkable efficacy. As therapeutic Tregs are being evaluated for treatment of autoimmune diseases and transplant rejection in humans, findings from this study will help to guide mechanistic studies associated with therapeutic Treg clinical trials and to identify adjunct therapies most likely to synergize with Tregs.

Supplementary Material

Refer to Web version on PubMed Central for supplementary material.

Acknowledgments

We thank V. Dang and N. Lescano for mouse husbandry; the UCSF BIDC for help with two-photon imaging; and Drs. J. A. Bluestone, J. G. Cyster, and A. Spence, all of UCSF, for helpful discussions and critical reading of this manuscript.

References

1. Tang Q, Bluestone JA. The Foxp3+ regulatory T cell: a jack of all trades, master of regulation. Nature immunology. 2008; 9:239–244. [PubMed: 18285775]
2. Kim JM, Rasmussen JP, Rudensky AY. Regulatory T cells prevent catastrophic autoimmunity throughout the lifespan of mice. Nature immunology. 2007; 8:191–197. [PubMed: 17136045]
3. Wing K, Onishi Y, Prieto-Martin P, Yamaguchi T, Miyara M, Fehervari Z, Nomura T, Sakaguchi S. CTLA-4 control over Foxp3+ regulatory T cell function. Science. 2008; 322:271–275. [PubMed: 18845758]
4. Pandiyan P, Zheng L, Ishihara S, Reed J, Lenardo MJ. CD4(+)CD25(+)Foxp3(+) regulatory T cells induce cytokine deprivation-mediated apoptosis of effector CD4(+) T cells. Nat Immunol. 2007; 8:1353–1362. [PubMed: 17982458]
5. Collison LW, Workman CJ, Kuo TT, Boyd K, Wang Y, Vignali KM, Cross R, Sehy D, Blumberg RS, Vignali DA. The inhibitory cytokine IL-35 contributes to regulatory T-cell function. Nature. 2007; 450:566–569. [PubMed: 18033300]
6. Mempel TR, Pittet MJ, Khazaie K, Weninger W, Weissleder R, von Boehmer H, von Andrian UH. Regulatory T cells reversibly suppress cytotoxic T cell function independent of effector differentiation. Immunity. 2006; 25:129–141. [PubMed: 16860762]
7. Tarbell KV, Petit L, Zuo X, Toy P, Luo X, Mqadmi A, Yang H, Suthanthiran M, Mojsov S, Steinman RM. Dendritic cell-expanded, islet-specific CD4+ CD25+ CD62L+ regulatory T cells restore normoglycemia in diabetic NOD mice. The Journal of experimental medicine. 2007; 204:191–201. [PubMed: 17210729]
8. Kendal AR, Chen Y, Regateiro FS, Ma J, Adams E, Cobbold SP, Hori S, Waldmann H. Sustained suppression by Foxp3+ regulatory T cells is vital for infectious transplantation tolerance. The Journal of experimental medicine. 2011; 208:2043–2053. [PubMed: 21875958]

9. Tang Q, Adams JY, Penaranda C, Melli K, Piaggio E, Sgouroudis E, Piccirillo CA, Salomon BL, Bluestone JA. Central role of defective interleukin-2 production in the triggering of islet autoimmune destruction. Immunity. 2008; 28:687–697. [PubMed: 18468463]
10. Chen Z, Herman AE, Matos M, Mathis D, Benoist C. Where CD4+CD25+ T reg cells impinge on autoimmune diabetes. The Journal of experimental medicine. 2005; 202:1387–1397. [PubMed: 16301745]
11. Tang Q, Henriksen KJ, Bi M, Finger EB, Szot G, Ye J, Masteller EL, McDevitt H, Bonyhadi M, Bluestone JA. In vitro-expanded antigen-specific regulatory T cells suppress autoimmune diabetes. The Journal of experimental medicine. 2004; 199:1455–1465. [PubMed: 15184499]
12. Tarbell KV, Yamazaki S, Olson K, Toy P, Steinman RM. CD25+ CD4+ T cells, expanded with dendritic cells presenting a single autoantigenic peptide, suppress autoimmune diabetes. J Exp Med. 2004; 199:1467–1477. [PubMed: 15184500]
13. Marek-Trzonkowska N, Mysliwiec M, Dobyszuk A, Grabowska M, Techmanska I, Juscinska J, Wujtewicz MA, Witkowski P, Mlynarski W, Balcerska A, Mysliwska J, Trzonkowski P. Administration of CD4+CD25highCD127− regulatory T cells preserves beta-cell function in type 1 diabetes in children. Diabetes care. 2012; 35:1817–1820. [PubMed: 22723342]
14. Tang Q, Adams JY, Tooley AJ, Bi M, Fife BT, Serra P, Santamaria P, Locksley RM, Krummel MF, Bluestone JA. Visualizing regulatory T cell control of autoimmune responses in nonobese diabetic mice. Nature immunology. 2006; 7:83–92. [PubMed: 16311599]
15. Feuerer M, Shen Y, Littman DR, Benoist C, Mathis D. How punctual ablation of regulatory T cells unleashes an autoimmune lesion within the pancreatic islets. Immunity. 2009; 31:654–664. [PubMed: 19818653]
16. Melli K, Friedman RS, Martin AE, Finger EB, Miao G, Szot GL, Krummel MF, Tang Q. Amplification of autoimmune response through induction of dendritic cell maturation in inflamed tissues. J Immunol. 2009; 182:2590–2600. [PubMed: 19234153]
17. Liu F, Whitton JL. Cutting edge: re-evaluating the in vivo cytokine responses of CD8+ T cells during primary and secondary viral infections. J Immunol. 2005; 174:5936–5940. [PubMed: 15879085]
18. Salomon B, Lenschow DJ, Rhee L, Ashourian N, Singh B, Sharpe A, Bluestone JA. B7/CD28 costimulation is essential for the homeostasis of the CD4+CD25+ immunoregulatory T cells that control autoimmune diabetes. Immunity. 2000; 12:431–440. [PubMed: 10795741]
19. Penaranda C, Tang Q, Ruddle NH, Bluestone JA. Prevention of diabetes by FTY720-mediated stabilization of peri-islet tertiary lymphoid organs. Diabetes. 2010; 59:1461–1468. [PubMed: 20299465]
20. Choi SE, Choi KM, Yoon IH, Shin JY, Kim JS, Park WY, Han DJ, Kim SC, Ahn C, Kim JY, Hwang ES, Cha CY, Szot GL, Yoon KH, Park CG. IL-6 protects pancreatic islet beta cells from pro-inflammatory cytokines-induced cell death and functional impairment in vitro and in vivo. Transplant immunology. 2004; 13:43–53. [PubMed: 15203128]
21. Suzuki T, Imai J, Yamada T, Ishigaki Y, Kaneko K, Uno K, Hasegawa Y, Ishihara H, Oka Y, Katagiri H. Interleukin-6 enhances glucose-stimulated insulin secretion from pancreatic beta-cells: potential involvement of the PLC-IP3-dependent pathway. Diabetes. 2011; 60:537–547. [PubMed: 21270264]
22. Carnaud C, Gombert J, Donnars O, Garchon H, Herbelin A. Protection against diabetes and improved NK/NKT cell performance in NOD.NK1.1 mice congenic at the NK complex. J Immunol. 2001; 166:2404–2411. [PubMed: 11160299]
23. Ogasawara K, Hamerman JA, Hsin H, Chikuma S, Bour-Jordan H, Chen T, Pertel T, Carnaud C, Bluestone JA, Lanier LL. Impairment of NK cell function by NKG2D modulation in NOD mice. Immunity. 2003; 18:41–51. [PubMed: 12530974]
24. Groom JR, Luster AD. CXCR3 ligands: redundant, collaborative and antagonistic functions. Immunology and cell biology. 2011; 89:207–215. [PubMed: 21221121]
25. Verdaguer J, Schmidt D, Amrani A, Anderson B, Averill N, Santamaria P. Spontaneous autoimmune diabetes in monoclonal T cell nonobese diabetic mice. The Journal of experimental medicine. 1997; 186:1663–1676. [PubMed: 9362527]

26. Nikolic T, Geutskens SB, van Rooijen N, Drexhage HA, Leenen PJ. Dendritic cells and macrophages are essential for the retention of lymphocytes in (peri)-insulitis of the nonobese diabetic mouse: a phagocyte depletion study. Lab Invest. 2005; 85:487–501. [PubMed: 15654358]
27. Saxena V, Ondr JK, Magnusen AF, Munn DH, Katz JD. The countervailing actions of myeloid and plasmacytoid dendritic cells control autoimmune diabetes in the nonobese diabetic mouse. J Immunol. 2007; 179:5041–5053. [PubMed: 17911589]
28. Onishi Y, Fehervari Z, Yamaguchi T, Sakaguchi S. Foxp3+ natural regulatory T cells preferentially form aggregates on dendritic cells in vitro and actively inhibit their maturation. Proc Natl Acad Sci U S A. 2008; 105:10113–10118. [PubMed: 18635688]
29. Tadokoro CE, Shakhar G, Shen S, Ding Y, Lino AC, Maraver A, Lafaille JJ, Dustin ML. Regulatory T cells inhibit stable contacts between CD4+ T cells and dendritic cells in vivo. The Journal of experimental medicine. 2006; 203:505–511. [PubMed: 16533880]
30. Villarino AV, Katzman SD, Gallo E, Miller O, Jiang S, McManus MT, Abbas AK. Posttranscriptional silencing of effector cytokine mRNA underlies the anergic phenotype of self-reactive T cells. Immunity. 2011; 34:50–60. [PubMed: 21236706]
31. Zheng Y, Collins SL, Lutz MA, Allen AN, Kole TP, Zarek PE, Powell JD. A role for mammalian target of rapamycin in regulating T cell activation versus anergy. J Immunol. 2007; 178:2163–2170. [PubMed: 17277121]
32. Rao RR, Li Q, Odunsi K, Shrikant PA. The mTOR kinase determines effector versus memory CD8+ T cell fate by regulating the expression of transcription factors T-bet and Eomesodermin. Immunity. 2010; 32:67–78. [PubMed: 20060330]
33. Araki K, Turner AP, Shaffer VO, Gangappa S, Keller SA, Bachmann MF, Larsen CP, Ahmed R. mTOR regulates memory CD8 T-cell differentiation. Nature. 2009; 460:108–112. [PubMed: 19543266]
34. Yao S, Buzo BF, Pham D, Jiang L, Taparowsky EJ, Kaplan MH, Sun J. Interferon Regulatory Factor 4 Sustains CD8 T Cell Expansion and Effector Differentiation. Immunity. 2013
35. Raczkowski F, Ritter J, Heesch K, Schumacher V, Guralnik A, Hocker L, Raifer H, Klein M, Bopp T, Harb H, Kesper DA, Pfefferle PI, Grusdat M, Lang PA, Mittrucker HW, Huber M. The transcription factor Interferon Regulatory Factor 4 is required for the generation of protective effector CD8+ T cells. Proc Natl Acad Sci U S A. 2013; 110:15019–15024. [PubMed: 23980171]
36. Man K, Miasari M, Shi W, Xin A, Henstridge DC, Preston S, Pellegrini M, Belz GT, Smyth GK, Febbraio MA, Nutt SL, Kallies A. The transcription factor IRF4 is essential for TCR affinity-mediated metabolic programming and clonal expansion of T cells. Nature immunology. 2013; 14:1155–1165. [PubMed: 24056747]
37. Powell JD, Pollizzi KN, Heikamp EB, Horton MR. Regulation of immune responses by mTOR. Annu Rev Immunol. 2012; 30:39–68. [PubMed: 22136167]
38. McNally A, Hill GR, Sparwasser T, Thomas R, Steptoe RJ. CD4+CD25+ regulatory T cells control CD8+ T-cell effector differentiation by modulating IL-2 homeostasis. Proc Natl Acad Sci U S A. 2011; 108:7529–7534. [PubMed: 21502514]
39. Penaranda C, Kuswanto W, Hofmann J, Kenefeck R, Narendran P, Walker LS, Bluestone JA, Abbas AK, Dooms H. IL-7 receptor blockade reverses autoimmune diabetes by promoting inhibition of effector/memory T cells. Proc Natl Acad Sci U S A. 2012; 109:12668–12673. [PubMed: 22733744]
40. Anderson MS, Bluestone JA. The NOD mouse: a model of immune dysregulation. Annu Rev Immunol. 2005; 23:447–485. [PubMed: 15771578]
41. Amrani A, Verdaguer J, Serra P, Tafuro S, Tan R, Santamaria P. Progression of autoimmune diabetes driven by avidity maturation of a T-cell population. Nature. 2000; 406:739–742. [PubMed: 10963600]
42. Coppieters KT, Dotta F, Amirian N, Campbell PD, Kay TW, Atkinson MA, Roep BO, von Herrath MG. Demonstration of islet-autoreactive CD8 T cells in insulitic lesions from recent onset and long-term type 1 diabetes patients. The Journal of experimental medicine. 2012; 209:51–60. [PubMed: 22213807]

43. Lee K, Nguyen V, Lee KM, Kang SM, Tang Q. Attenuation of donor-reactive T cells allows effective control of allograft rejection using regulatory T cell therapy. Am J Transplant. 2014; 14:27–38. [PubMed: 24354870]

44. Gasteiger G, Hemmers S, Bos PD, Sun JC, Rudensky AY. IL-2-dependent adaptive control of NK cell homeostasis. The Journal of experimental medicine. 2013

45. Gasteiger G, Hemmers S, Firth MA, Le Floc'h A, Huse M, Sun JC, Rudensky AY. IL-2-dependent tuning of NK cell sensitivity for target cells is controlled by regulatory T cells. The Journal of experimental medicine. 2013

46. Sitrin J, Ring A, Garcia KC, Benoist C, Mathis D. Regulatory T cells control NK cells in an insulitic lesion by depriving them of IL-2. The Journal of experimental medicine. 2013

47. Chang CH, Curtis JD, Maggi LB Jr, Faubert B, Villarino AV, O'Sullivan D, Huang SC, van der Windt GJ, Blagih J, Qiu J, Weber JD, Pearce EJ, Jones RG, Pearce EL. Posttranscriptional control of T cell effector function by aerobic glycolysis. Cell. 2013; 153:1239–1251. [PubMed: 23746840]

48. Vignali DA, Collison LW, Workman CJ. How regulatory T cells work. Nature reviews. Immunology. 2008; 8:523–532.

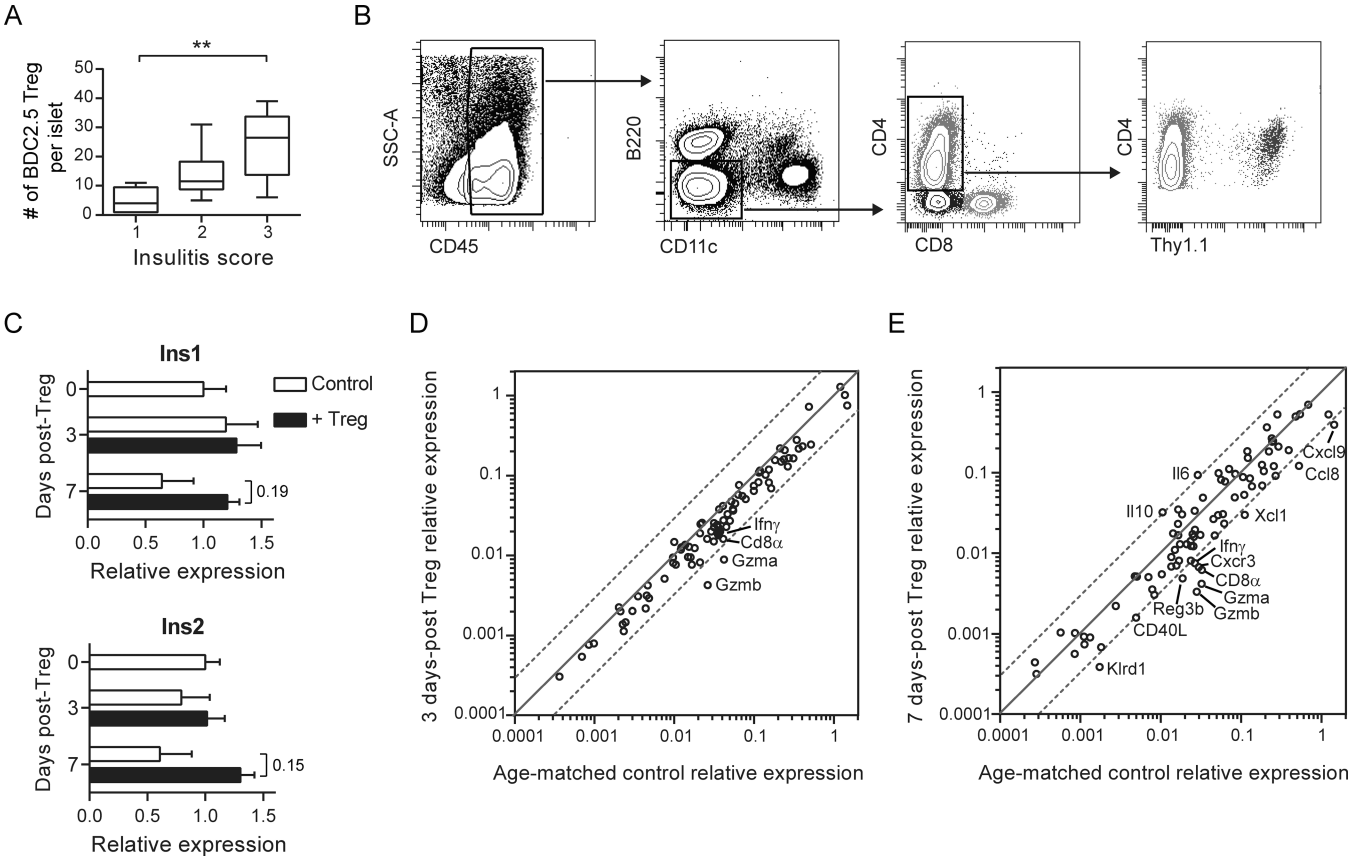

Fig. 1.

Tregs traffic to inflamed islets where they down-regulate an effector T cell signature. (**A**) BDC2.5 Tregs were enumerated in isolated NOD.CD11c-YFP.CD28$^{-/-}$ islets scored for insulitis using two-photon microscopy at 1 to 7 d post-Treg transfer. Insulitis score 1 = minimal infiltrate; 2 = infiltrate confined to <50% of islet; 3 = infiltrate covering >50% of islet. Box whiskers represent min to max of 6–8 islets per group analyzed over 2 independent experiments. Kruskal-Wallis test followed by Dunn's post test, **, $P < 0.01$. (B) BDC2.5 Tregs and immune infiltrates persist in the islets following Treg treatment. Flow cytometry plots depict the gating strategy for various immune cell populations in the islets of a NOD.CD28$^{-/-}$ mouse 2 weeks post-transfer of Thy1.1^{+} BDC2.5 Tregs. Within islet single cell suspensions, immune infiltrates were gated as CD45^{+}. APCs were excluded by gating on B220^{-}CD11c^{-} cells, and then CD4^{+} and CD8^{+} T cells were gated from this double negative population. Transferred BDC2.5 Tregs were identified among CD4^{+} T cells by their expression of Thy1.1. (**C–E**) mRNA was isolated from islets pooled from 4–5 NOD.CD28$^{-/-}$ mice at the time of Treg transfer and at 3 and 7 d after Treg treatment. (**C**) Expression of insulin 1 and 2 at day 0, 3, and 7 post-Treg treatment, normalized to time of treatment baseline. Data represent the average from 2 independent experiments. Bar graphs display mean ± SEM. P values (shown for day 7 treated vs. untreated) were determined using the Holm-Sidak method for multiple t tests. (**D, E**) Scatter plots displaying the relative abundance of mRNA transcripts in NOD.CD28$^{-/-}$ islets at 3 d (**D**) and 7 d (**E**) following

Treg treatment, as compared to age-matched controls. Dashed lines represent a 3-fold difference between groups. Data are from 2 independent experiments.

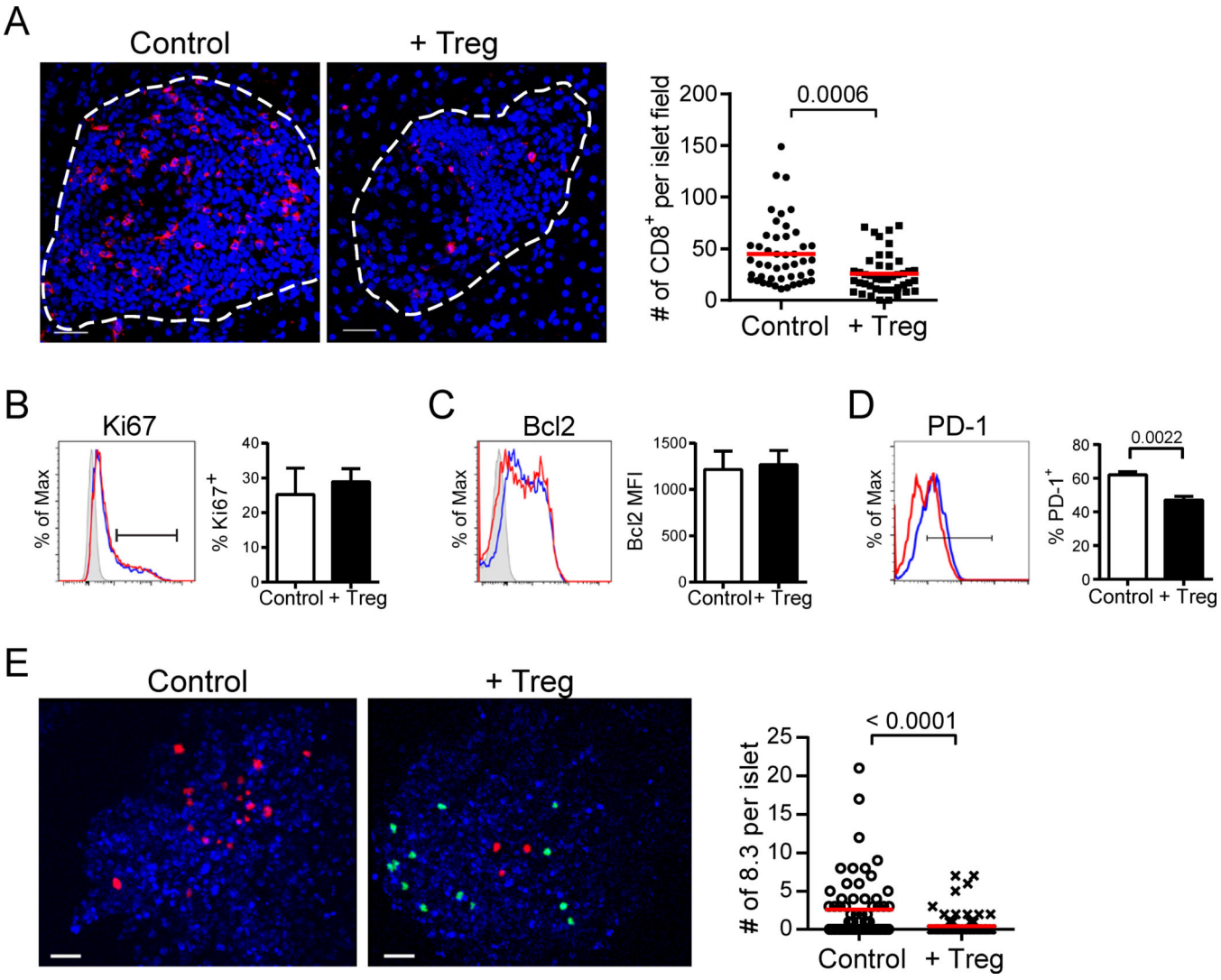

Fig. 2.

Tregs reduce $CD8^+$ T cell accumulation in the islets. (**A**) Representative immunofluorescence images showing infiltrated islets of control and 7 d post-Treg treatment NOD.$CD28^{-/-}$ mice. $CD8^+$ T cells are shown in red and nuclei are blue. Dashed lines outline the islets. Scale bars represent 30 μm. Graph depicts the number of $CD8^+$ cells per islet section. Each dot represents one islet. Data are from over 40 islets analyzed from 3 mice per group. Red lines represent mean. P value was determined by Mann-Whitney test. (**B–D**) Islets were isolated from NOD.$CD28^{-/-}$ mice at 7 d post-Treg treatment and from age-matched controls for analysis by flow cytometry. Histograms overlay expression levels of Ki67 (**B**), Bcl2 (**C**), and PD-1 (**D**) in islet $CD8^+$ T cells of Treg-treated (red) and control (blue) mice. $CD8^+$ T cells were gated as viability $dye^-Thy1.2^+CD8^+$. Shaded peaks in B and C represent isotype control stains. Bar graphs depict the percent $Ki67^+$ (**B**), the median fluorescence intensity (MFI) of Bcl2 (**C**), and the percent $PD\text{-}1^+$ (**D**) for islet $CD8^+$ T cells. Data represent the mean ± SEM of 6 mice per group from 2 independent experiments. P values were determined by Mann-Whitney test with no statistically significant differences

observed for B or C. (**E**) 10^7 CMTMR-labeled 8.3 $CD8^+$ T cells were transferred to NOD.$CD28^{-/-}$ mice at 7 d post-uGFP.BDC2.5 Treg treatment and to untreated littermate controls. Islets were harvested the following day, labeled with Hoechst, and imaged by two-photon microscopy. Representative maximal projection images show a control and Treg-treated Hoechst-labeled islet (blue) containing 8.3 $CD8^+$ T cells (red) and BDC2.5 Tregs (green, + Treg only). Scale bars represent 30 μm. Graph quantifies the number of 8.3 $CD8^+$ T cells per islet. Each dot represents one islet. Data are from 2 independent experiments with greater than 60 islets analyzed per group. Red lines represent mean. P value was determined by Mann-Whitney test.

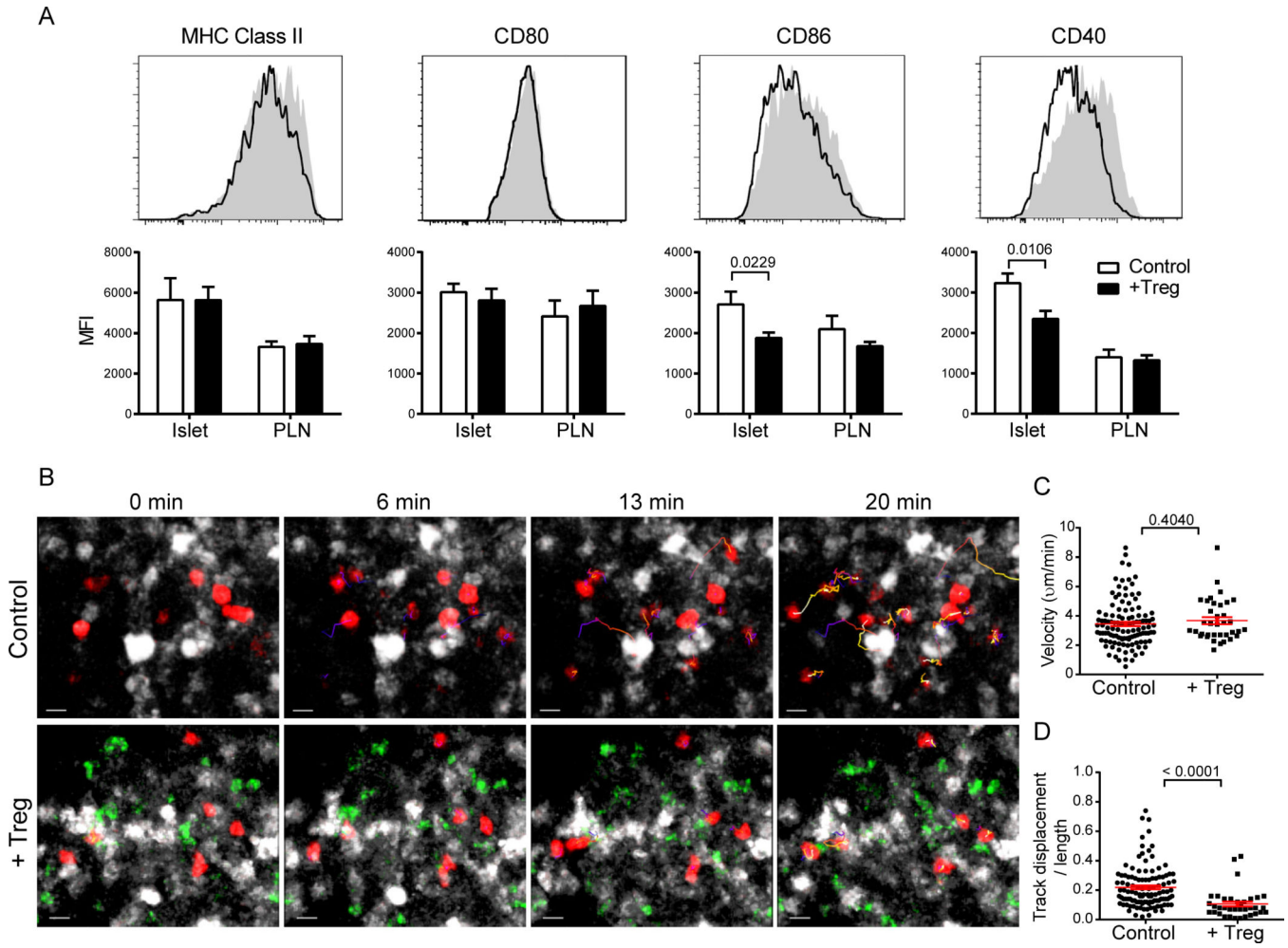

Fig. 3.

Treg treatment does not inhibit islet T cell-DC interactions. (**A**) Histograms depict expression levels of the indicated molecules on islet DCs of age-matched control (shaded) and 7 d post-Treg-treatment (outline) NOD.CD28$^{-/-}$ mice. DCs were gated as CD45^{+}CD11c^{+}B220^{-}DAPI^{-}. Bar graphs depict median fluorescent intensities. Data represent mean ± SEM of 6–10 mice per group from 2–3 independent experiments. P values were determined by Mann-Whitney test. (**B–D**) 10^{7} CMTMR-labeled 8.3 CD8^{+} T cells were transferred to NOD.CD11c-YFP.CD28$^{-/-}$ mice at 7 d post-uGFP.BDC2.5 Treg treatment and to untreated controls. Islets were harvested the following day and imaged by two-photon microscopy. (**B**) Maximal projection time-lapse images from control and Treg-treated islets depicting CD11c^{+} DCs (white), 8.3 CD8^{+} T cells (red), and BDC2.5 Tregs (green, + Treg only). Track lines depict 8.3 CD8^{+} T cell movements over the course of the 20 min imaging period and are color-coded according to time (blue at the beginning of the imaging period to white at the end). Scale bars represent 10 μm. See Supplemental Videos 2 and 3 for full time lapses. (**C, D**) Graphs depict velocities (**C**) and confinement ratios (**D**) of 8.3 CD8^{+} T cells. Each point represents a single cell; red bars represent mean ± SEM. Data are from multiple islets imaged over 2 independent experiments. P values were determined by Mann-Whitney test.

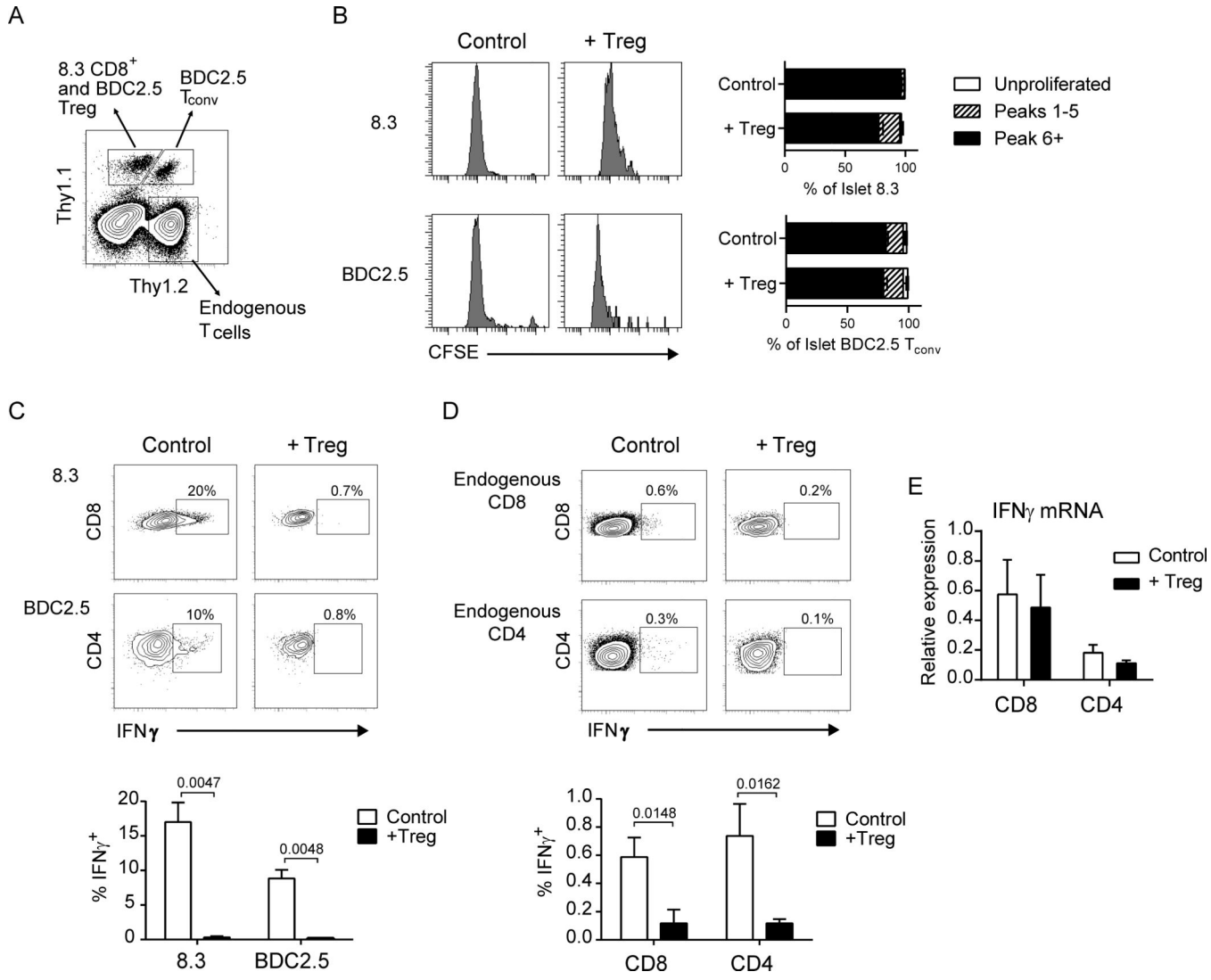

Fig. 4.

Tregs suppress islet T cell effector function. (**A–D**) 10^6 CFSE-labeled 8.3.Thy1.1$^+$ CD8$^+$ T cells and BDC2.5.Thy1.1$^+$Thy1.2$^+$ CD4$^+$CD25$^-$ T cells were transferred to NOD.CD28$^{-/-}$ mice 3 d following BDC2.5.Thy1.1$^+$ Treg treatment or to untreated littermates and analyzed 4 d later. (**A**) Representative flow plot depicting gating of endogenous and transferred T cells. Cells were pre-gated as CD45$^+$ lymphocytes. Transferred 8.3 CD8$^+$ T cells and BDC2.5 Tregs were gated as Thy1.1$^+$Thy1.2$^-$ and were further differentiated based on CD8 and CD4 expression. BDC2.5 conventional CD4$^+$ T cells were Thy1.1$^+$Thy1.2$^+$. Endogenous T cells were Thy1.2$^+$Thy1.1$^-$ (**B**) Representative histograms pre-gated on Thy1.1$^+$ CD8$^+$ 8.3 T cells and Thy1.1$^+$Thy1.2$^+$CD4$^+$ BDC2.5 T cells depicting CFSE dilution of transferred cells in the islets with and without Treg treatment. Bar graphs depict the percentage of cells that did not divide (Unproliferated), underwent 1–5 rounds of division (Peaks 1–5), or underwent 6 or more rounds of division (Peak 6+). Kruskal-Wallis test followed by Dunn's post test, *, $P < 0.05$. (**C**) Representative flow plots pre-gated on 8.3 CD8$^+$ (top) and BDC2.5 T_{conv} (bottom) cells showing IFNγ expression by intracellular flow

cytometry. Bar graph depicts summary data from 6 mice per group from 2 independent experiments. (**D**) Representative flow plots pre-gated on endogenous islet $Thy1.2^{+}Thy1.1^{-}$ $CD8^{+}$ (top) and $CD4^{+}$ (bottom) T cells and quantification of the percent expressing intracellular $IFN\gamma^{+}$. Bar graph depicts summary data as in C. Bar graphs depict mean ± SEM. P values for C and D were determined by Mann-Whitney test. (**E**) qRT-PCR data measuring transcript levels of IFNγ for $CD8^{+}$ and $CD4^{+}$ T cells sorted from pooled islets of 3–4 NOD.$CD28^{-/-}$ mice at 7 d post-Treg treatment or from age-matched controls. Expression levels are normalized to 18s rRNA expression. Data are represented as the mean ± SEM of 4 independent experiments. No statistically significant difference was observed between control and Treg-treated samples by Wilcoxon matched-pairs signed rank test.

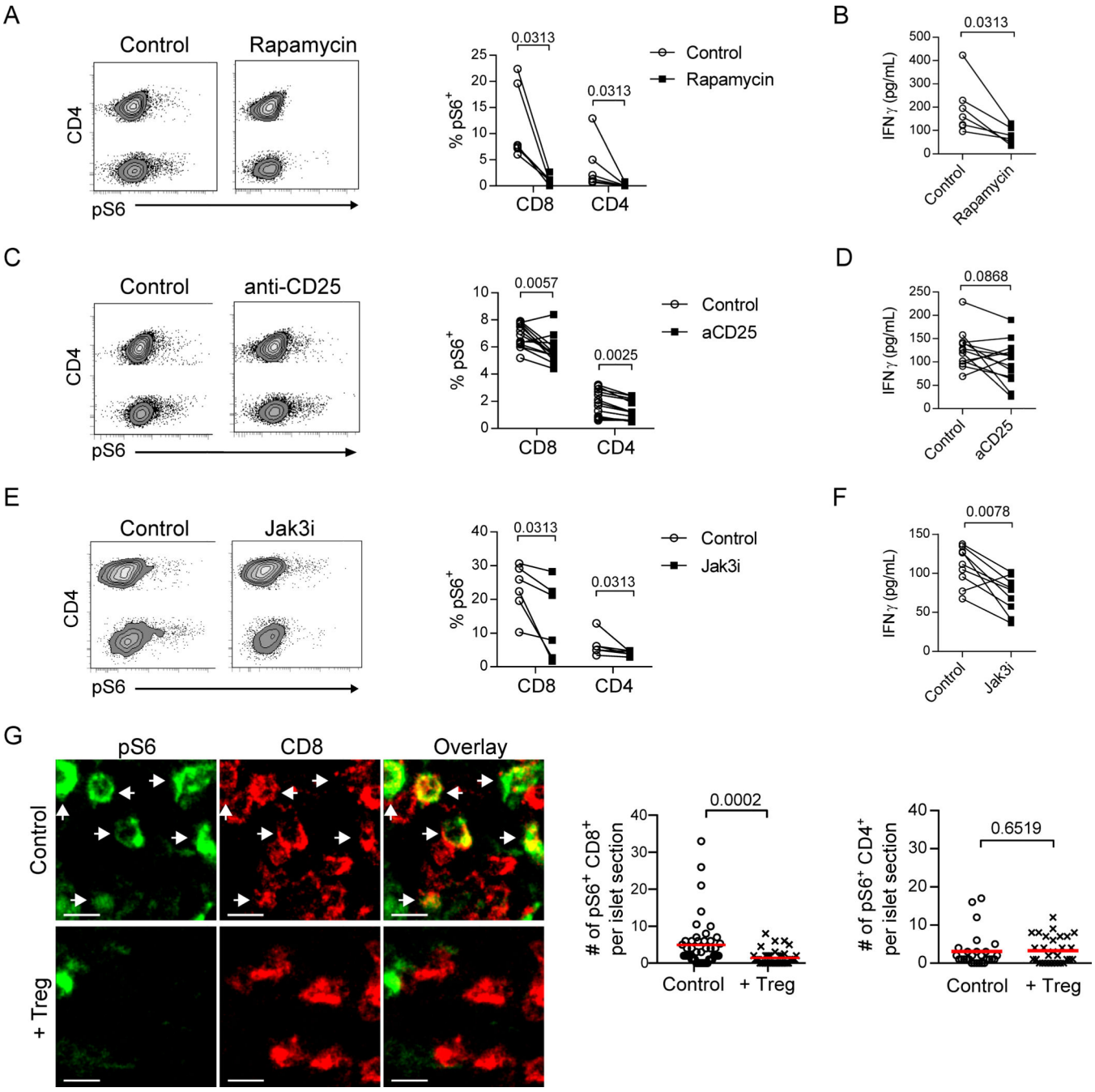

Fig. 5.

Tregs suppress mTOR signaling in islet $CD8^+$ T cells that is critical for IFNγ production. (**A, C, E**) Representative flow plots showing T cells from isolated islets of NOD.$CD28^{-/-}$ mice that were dissociated and cultured overnight in the presence or absence of rapamycin, anti-CD25 antibody, or Jak3 inhibitor. Depicted T cells were gated as viability $dye^-CD45^+CD11c^-B220^-Thy1.2^+$. CD4 expression on the y-axis of the flow plots separates $CD4^+$ T cells on the upper half of the plot from $CD8^+$ T cells on the lower half. Graph depicts the mean percent of T cells expressing pS6 ± SEM. (**B, D, F**) Concentrations of

IFNγ in culture supernatants were determined by ELISA. Each connected pair of data points represents cells from one mouse. Data for A–F are from 2–3 independent experiments. P values were determined by Wilcoxon matched-pairs signed rank test. (**G**) Representative immunofluorescence images of stained pancreas sections from NOD.CD28$^{-/-}$ mice at 7 d post-BDC2.5 Treg treatment or from untreated littermates. pS6 signal is indicated in green and CD8^{+} T cells are shown in red. White arrows highlight co-expression. Scale bars represent 10 μm. Graphs quantify the number of CD8^{+} T cells (left) or CD4^{+} T cells (right) per islet section expressing pS6. Data are combined from 3 independent experiments with a total of 3 mice for each condition. Each point represents an individual islet; red lines indicate the mean. P values were determined by Mann-Whitney test.

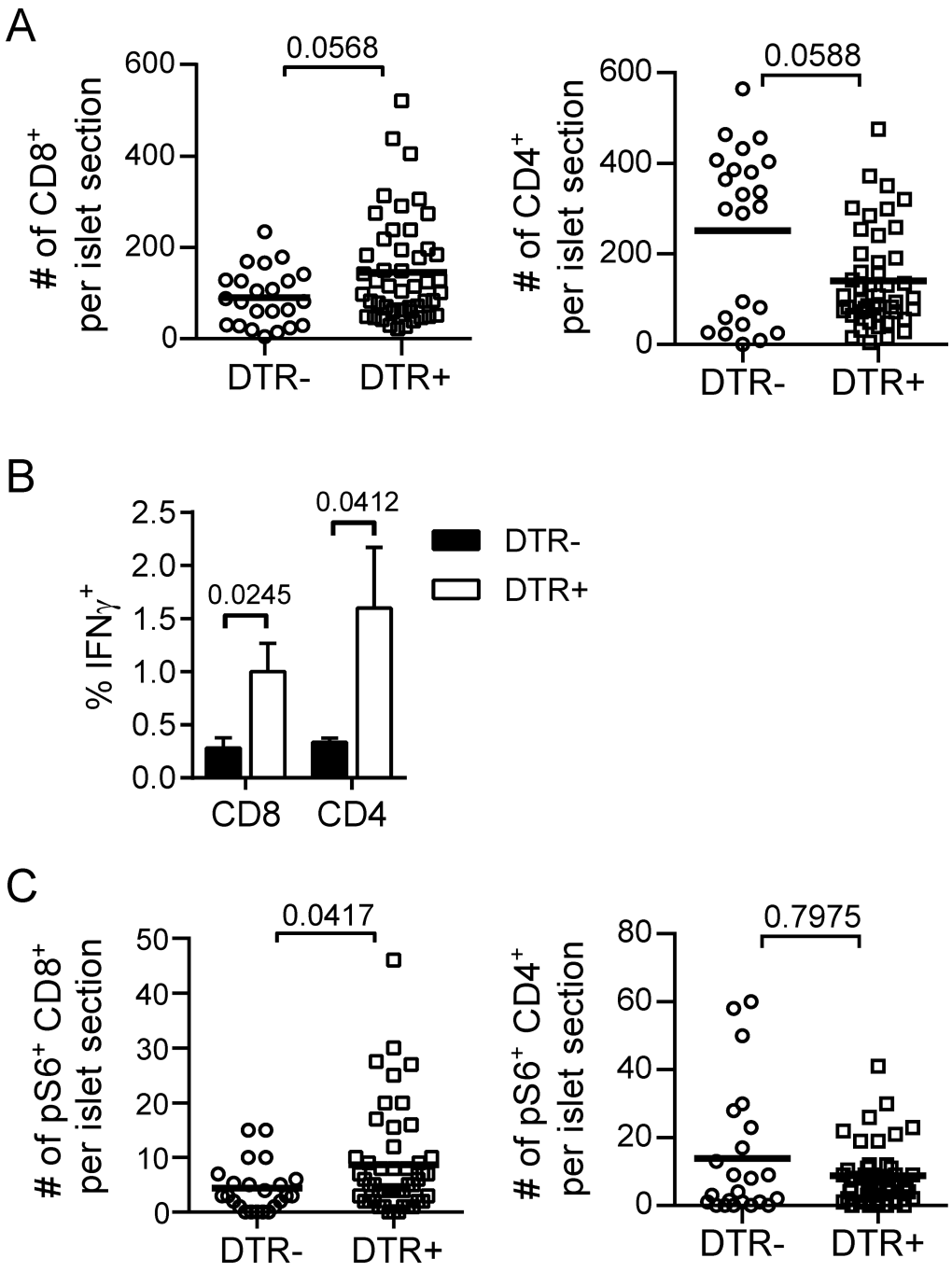

Fig. 6.

Treg depletion in NOD mice enhances islet T cell effector function, $CD8^+$ T cell numbers and mTOR activation. NOD.Foxp3^{DTR+} mice and transgene-negative littermate controls were sacrificed for analysis following 2 d of DT treatment. (**A**) Numbers of $CD8^+$ T cells (left) and $CD4^+$ T cells (right) per islet section were quantified by immunofluorescence microcopy. (**B**) Islet T cell IFNγ production was determined by *ex vivo* intracellular cytokine staining as in Figure 4. Data are from 6 mice per group combined from 2 independent experiments. Bar graph depicts mean ± SEM. (**C**) Numbers of $pS6^+$ $CD8^+$ T cells (left) and

pS6^{+} CD4^{+} T cells (right) per islet section were quantified by immunofluorescence microcopy. Data for A and C are combined from 2 independent experiments with a total of 3–5 mice for each condition. Each point represents an individual islet; bold lines indicate the mean. P values were determined by Mann-Whitney test.